Detection of Energetic Particles from Plasma Focus using Faraday Cup and SSNTD (LR-115A)

G.M.El-Aragi

Plasma Physics and Nuclear Fusion Dept., Nuclear Research Center, AEA, P.O. Box 13759 Cairo, Egypt

Abstract. A Mather-type plasma focus device is used in this work which is prefilled with helium at 0.8 Torr. The total ion current density of the plasma stream is measured to be 750 mA/cm^2 . From time-resolved measurements (Faraday cup), the ion beam energy was distributed with energy ranging from 0.3 keV to 540 keV. The ion flux density of ion beam is estimated to be 4.47×10^{11} ion/steradian using track etching techinque (LR-115A).

Keywords: energetic ions, plasma focus, charging voltage

PACS: 52.59.Hq

Introduction

Ion diagnostics of high-temperature plasma objects are considered to be very important, because they provide essential data about plasma parameters. Ion beams are emitted from the high-temperature plasma objects are an abundant source of valuable information about fusion reaction yields, plasma ion temperatures, as well as a spatial distribution of fusion reaction sources.
In several theoretical papers [1,2,3] very simple configurations have been adopted to explain ion behavior inside of the plasma column.
Experimental studies of Dense Plasma Focus (DPF) facilities proved the occurrence of high-energy ion beams, generated within the plasma focus pinch column or its vicinity.
High energetic ions are considered to play an important role in the production of the intense neutron flux in the plasma focus device when using deuterium gas [4].
Studies of high-energy ions emitted from plasma focus devices provide information on the ion acceleration mechanisms and are also important for various plasma focus technology. Gerdin et al [5] employed a Faraday cup in a time-of-flight technique to measure the ion spectrum and a careful study of the ion-neutral interactions allowed the observation of deuteron energies down to ~ 25 keV. Different kinds of acceleration mechanisms for charge particle were identified [6,7]. General characteristics of the ion beams were studied in different laboratories [8,9].
The Plasma Focus (PF) is a device consisting in two coaxial electrodes in vacuum connected to a fast high voltage capacitor bank and separated by an insulator. When the HV is applied to the electrodes through a thyratron switch, an electrical breakdown develops on the surface of the insulator and the discharge is driven by the Lorentz force to run along the gap between the electrodes at a speed of some 10^6 cm/s and when reaches the end of the inner electrode collapses on the axis of the device focusing in a hot blob of plasma (Plasma Focus). In this phase strong electric fields are generated that produce intense ion beams. The duration of each discharge is of the order of 8 μs.

Experimental setup

Mather-type 112.5 J plasma focus device consists of an outer electrode, which is formed of eight copper rods, each of 130 mm length and 10 mm diameters as shown in figure 1. The outer diameter of center electrode is 18 mm and inner diameter of squirrel cage (outer electrode) is 55 mm. A hole of 5 mm diameter and 8 mm depth was drilled in the

front of the inner electrode in which different metals were filled. The cylindrical insulator ring is of 130 mm diameter and 35 mm thickness. The electrode system is enclosed in a vacuum chamber made of stainless steel tank of 350 mm length and 100 mm diameter. There are several ports in the vacuum chamber for diagnostic purposes. The condenser bank of plasma focus device consists of one condenser of 25 kV and 1 μF low inductance condenser. A capacitor bank charged at 15 kV (112.5 J), giving peak discharge current of about 5 kA, powered the focus device.
The inner electrode is connected to the positive connection of high voltage supply via a triggertron-type vacuum tube (CX1159) served as a switch, whereas the outer electrode is grounded.

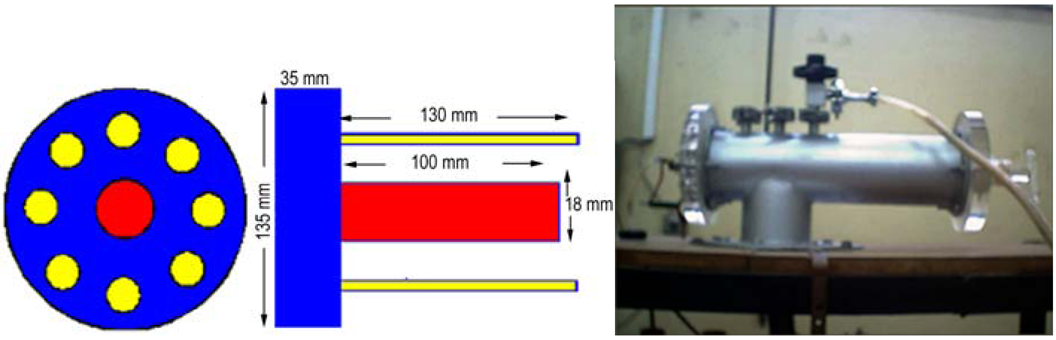

Fig. 1. Schematic of experimental setup

The vacuum chamber was evacuated up to 10^{-2} mbar pressure by a rotary pump (Edwards single stage model 1 Sc.-150B) before filling gas (helium). To avoid vapor from back streaming, the vacuum chamber is washed by gas after evacuation by rotary pump. The gas was fed into the system via flow meter (OMEGA model). The circuit diagram of trigger pulse for plasma discharge is shown in figure 2. The external inductance of the system including the capacitor, thyratron switch, connecting cables and coaxial electrodes (cathode and anode) is measured to about 6.5 μH.

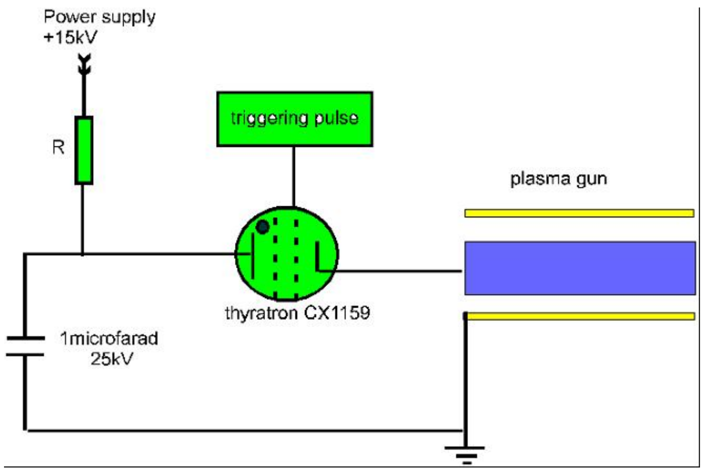

Fig. 2. The circuit diagram of trigger pulse

In order to register the particle radiation within the pinhole camera, the use was made of nuclear track detectors of the LR-115A type. After irradiation those detectors were etched under standard conditions (in a 6.25-N solution of NaOH, at a temperature of 70^{o}C) for a period ranging from one hour to several hours. To perform time-resolved measurements there were used Faraday-type collectors: a single cup (FC) and a so-called double-cup system (DFC), which used two ring-shaped collectors placed at a given distance (time-of-flight basis), but adjusted along the common z-axis.
The applied voltage to and the discharge current through the discharge chamber were measured using a voltage divider (Home made), which was connected between the two electrodes, and a current monitor, which can be located upon returning to the ground. The signals from the voltage divider and the current monitor were recorded in a digitizing oscilloscope (Lecroy, USA) with a 200-MHz bandwidth.
The peak value of the discharge current was measured is approximately 5 kA during the pulse. Figure (3) shows the current and voltage waveforms that characterized the pulsed low energy plasma focus device. Current and voltage were measured as a function of time at an input energy of 112.5 J (maximum applied voltage 15kV).

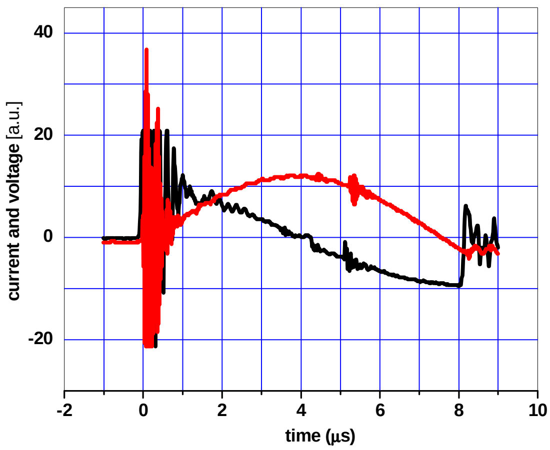

Fig. 3. Discharge current (red) and voltage (black) signals from the plasma device.

Results and Discussion

When an ion penetrates into the background of neutral gas, it loses energy by collisions, some of these ions attenuate and other stops at certain distance L Faraday cup- plasma focus. This distance depends on the ion mass, ion energy, nature and density of the neutral gas. The energy transform from the ion beam to the bulk of neutral gas is considered as an energy flux released in layers of the gas i.e. part or whole kinetic energy of the ions is transformed into thermal energy into the bulk of the gas.
Also, the neutral gas broadens the beam through multiple scattering i.e. lateral spread of the beam. As well as, the beam particles capture and lose electrons to the gas to form an equilibrium charge state.
The passage of the beam through the background gas between the focus and the Faraday cup has three major influences on the beam properties. These are:
1- The neutral gas removes energy from the beam particles i.e. the energy attenuation of the beam.
2- The neutral gas broadens the beam through multiple scattering i.e. lateral spread of the beam.

3- The beam particles capture and lose electrons to the gas to form an equilibrium charge state.
The accelerated ion beams have a conic geometry with solid angle θ, the Faraday cup receive an effluence which depend on the distance between focus and Faraday cup.
Preliminary time-resolved measurements of the ion pulses were carried out by means of an ion collector, which was placed at a distance of 20 cm from the top of the anode. The ion collector consists of a copper disc of 2.0 cm diameter which is connected to the ground through resistor (R =75 mΩ). The voltage develop across the resistor is fed it digital storage oscilloscope (Lecroy) to record the ion current signals. The collector plate was polarized negatively, and the whole measuring circuit was shielded against electromagnetic noise. Time-resolved studies of ions were performed by means of a double-collector of the Faraday type, which was designed especially for TOF measurements of pulsed charged-particle streams. That detector was equipped with two separate collectors (collector and grid) adjusted along the same Z-axis. The first ring-shaped collector (grid) was placed at a distance of 20 cm from the focus pinch, and the second one was situated about 2 cm behind the first collector. Some examples of the registered traces of the collector signals are presented in Fig. 4

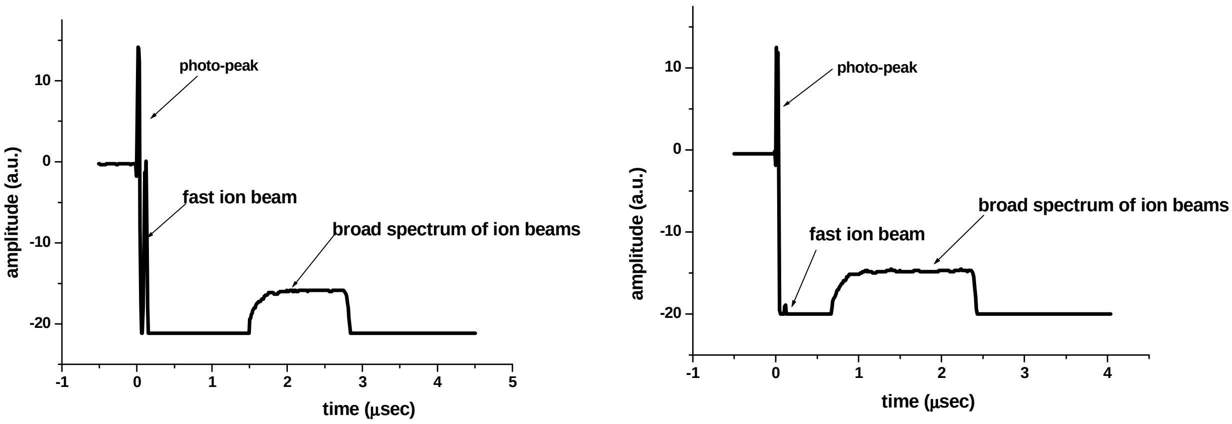

Fig. 4. Typical Faraday cup signals obtained from a single discharge left signal (a) indicate good peak of fast ions while right signal shows much smaller fast ions than right one (b).

The velocity, energy and density of helium ions are estimated using TOF technique [10,11]. The ion velocity is estimated by taking the ratio of the distance to the flight time of ions from source to detector.
The variation of ion flux with fillig helium gas pressure is shown in figure (5). It is note that the maximum ion flux reaches at maximum value at pressure 0.8 Torr, consquantly the best operating pressure for ion detection in this experiment is 0.8 torr.

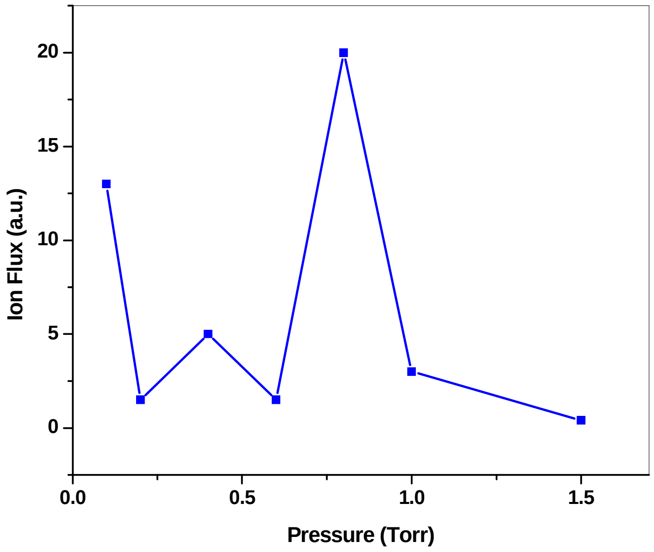

Fig. 5. Variation of ion flux with helium gas pressure (Torr)

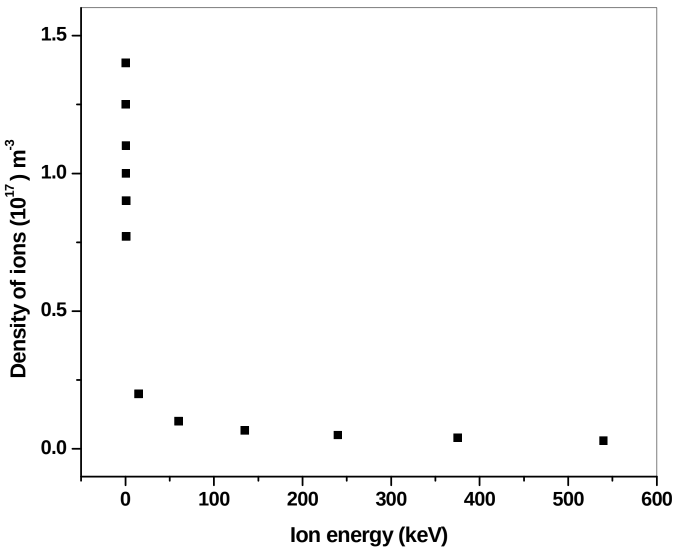

Fig. 6. Energy specrum of ion

The energy spectrum of helium ion is shown in figure (6). Data shows two groups of ion spectrum, first group of lower kinetic energy corresponding to helium ion with kientic energy ranging from 0.3 to 1.0 keV, and second group of higher kientic value ranging from 15 to 540 keV.

Track etching technique has been successfully employed in many insulating materials for detection and identification of charged particles, e.g. in the study of heavy primary cosmic rays, the search for super heavy elements and innumerable applications in radiation dosimeters. Early in the past decade cellulose nitrate as recognized as the most sensitive of all track detectors, and so has been used as a detector to record protons.

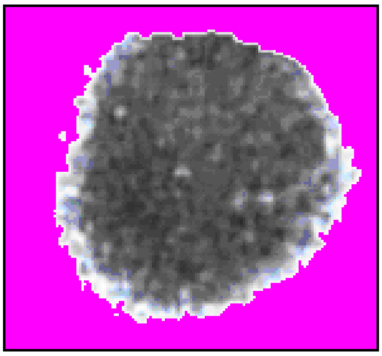

Fig. 7. Image of the helium ion tracks (0.8 torr, 15 kV) as obtained from plasma focus discharge with LR-115A film.

The ion beam of the present image has a circular cross-sectional area 28 μm^2 . The beam contain a large number of fast ions which are distributed uniformally or quasiuniformally over the beam cross-section. A majority of quasi-uniform ion density, where the density of ions is is distributed in an increasing trend toward the beam center.
It is possible to estimate the ion flux density of microbeam using a model consisting of a core surrounded by co-central zones (CCZ model) is proposed [13]. The registered ion images are obtained for 0.1 J/ 15 kV PF-shots performed at the initial filling gas pressure P = 0.8 Torr helium. The total ion emission (centerd on Z-axis) is estimted to be 4.47 $\times 10^{11}$ ion/steradian.
The shear in the velocity in conjunction with B_θ will produce centrifugal force which tends to a rotary or vortex pattern. Once the vortex or vortices are setup, the acceleration of plasma is the centrifugal acceleration which is provided by currents flowing in the direction of rotary motion of the mass of the plasma. The rotational drift velocity is greater for the ions because of their greater mass and hence a net circular current flows will crossed with B_θ to produce a centrifugal acceleration to hold the plasma in the form of an eddy or vortex.
The drift velocity of ions due to viscous forces in rotating plasma provide an azimuthally current density J_θ and an axial magnetic field B_z. The B_z field due to such viscous battery is proportional to the vortices of the fluid. The rotational velocity V_θ is composed of three drifts i.e. $E \times B$ drift, diamagnetic drift and centrifugal force drift. The plasma is accelerated not only axially by $J_z \times B_\theta$ force but azimuthally by $J_\theta \times B_z$ force, where J_z is the axial discharge current and B_θ is self-induced azimuthally magnetic field.

Acceleration Mechanism
In the radial phase, shock front and the piston starts together at r=a length of the pinch is zero at this time. In any plane the velocity of the shock front is larger than the piston velocity, so the distance between them is a time dependent quantity. The shock front accelerates onto the axis, hitting it; a reflected shock develops and moves in radial outwards (figure 8). The piston continuous to compress inward until it hits the outgoing reflected shock front. The meeting point between reflected shock and a piston called point of maximum compression of the pinch (minimum radius). The dimension and lifetime of the pinch dependent on the radius of the anode.

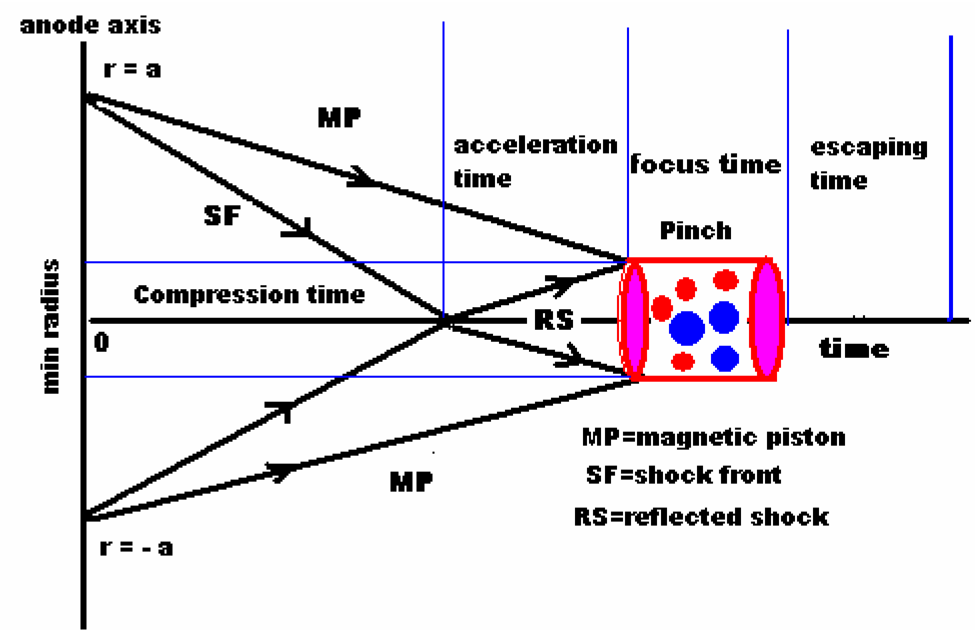

Fig. 8. Schematic of radial phase development when magnetic piston separates from

Compression phase start after transformation of plasma structure to plasma column. This plasma column will compressed adiabatically to form the pinch of final focus. The rapid compression of relatively dense plasma leads to heating plasma to a thermonuclear (fusion) temperature. The plasma collapses toward the center with approximately constant acceleration and flutes which subsequently develop on the outer surface of the plasma are interpreted as Rayleigh-Taylor.

Rayleigh-Taylor instability prevents the compression of the plasma column to get uniformly radial. The magnetic field starts diffusing into the plasma column, leading to an anomalous high plasma resistance as well as increasing the inductance of the system because of increasing the density of plasma column. The sharp change in plasma inductance and high plasma resistance induces high electric field inside the plasma column. This electric field will accelerate the ions and electrons in opposite direction. As result for that, the relative drift between ions and electrons leads to an increasing electron thermal velocity.

If the density clump occurs in plasma, an electric field can cause the ions and electrons to separate, generating another electric field. If there is feedback mechanism that causes the second electric field to enhance the first one, an electric field grows indefinitely and the plasma is unstable. Such instability called drift instability. In some cases, drifts can be self-perpetuating (charge separation leading to a drift, leading to more charge separation and so on), so that plasma instability results.

Generation of high energy particles and radiation in the plasma focus are considered to be an indication of non-thermodynamic equilibrium of the pinch. The presence of a beam of charged particles that forms in the plasma is explained by the appearance of electric fields which can be caused by the development of a Rayleigh-Taylor instability, plasma turbulence, magneto-acoustic wave propagation in the pinch.

In plasma focus, especially in the pinch phase the plasma gets more compressed at the onset of hydrodynamic instabilities (m = 0) as shown in figure (9). The charged particles (ions and electrons) are trapped between two layers of plasma current sheath which acts like two moving magnetic mirrors with radius R and these particles initially have a velocity V_i .

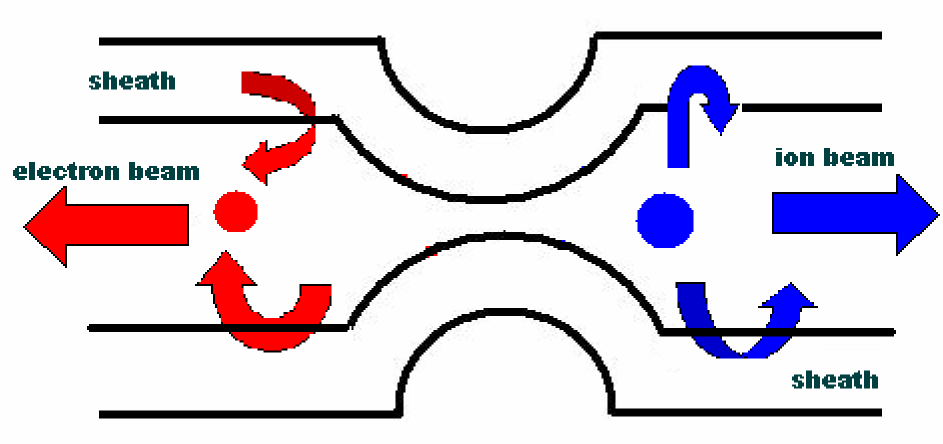

Fig. 9. Shows the plasma pinch and emission beams of charged particles onset of instability inducing micro instabilities.

YOUSEFI et al, were observed in the plasma column, a ring-shape around the dense plasma column (necking) that it can be attributed to the ion shape in the pinhole image. In fact, it seems that, m = 0 instability (necking) cause the ions acceleration with periods of few to tens of nanoseconds.

During compression phase the plasma density is high, then coulomb collisions between electrons and ions will efficiently thermalise the plasma. The dissipated energy ends up distributed equally amongst the particles, forming a Maxwellian distribution. The particles are accelerated in the current sheath medium as result of many collisions which act as a scattering center. Here the charged particles impinging on the oscillating sheath edge suffer a change of a velocity upon reflection back into the bulk plasma. As the sheath moves into the bulk, the reflected particles gain energy, as the sheath moves away, the particles lose energy. As the particle goes deeper into the sheath which acts as a potential barrier, it is slowed down by the retarding space charge field. After it has entirely lost its velocity, it turns back and increases its velocity under the action of an accelerating field, returning to the plasma.

In a coordinate system related to the moving plasma boundary, the particle experiences purely elastic recoil. By using the loss cone formula and the invariance of μ the energy to which the charged particle will accelerated before it escape. The plasma boundary can be treated as flat piston and the particle has a velocity $V_i > 0$ and hit the piston moving at velocity $V_P < 0$. In the frame of the piston the particle bounces elastically and comes off with its initial velocity, but in the opposite direction. By transforming back to the laboratory frame the velocity of the recoil particle V_f is given by

$$V_f = - V_i + 2 V_P$$

And its kinetic energy on recoil changes to

$$\Delta\varepsilon = -2m V_P (V_i - V_P)$$

At each bounce, the change in momentum is

$$\delta P = 2M |V_P|$$

where M is mass of particle, and let the number of bounces N
At a given values of V_i and $|V_P|$, the recoil particle gain energy if the potential barrier moves to meet the charge particle ($V_i > 0 > V_P$). If the particle overtakes the potential barrier ($V_i > V_P > 0$), it loses its energy on the recoil.
Then the number of bounces depend on the initial velocity of the particle (initial momentum) and the piston velocity and given by

$$N = V_i / 2 V_P$$

The statistical net gain in energy results from collisions of particles off centers.
It is then easy to see that in this case the particle would be trapped between moving plasma boundary (the boundary acts as a potential barrier), an effect appropriately called trapping. The potential barrier then act exactly likes the ping-pong paddles, scattering the particle back and forth as the two plasmas converge. This causes that particle to gain momentum and, subsequently, be accelerated.
After all, a particle can't be accelerated infinitely; it has to be ejected from the system eventually. There are two important quantities at work here; the acceleration timescale and the escape timescale. These two work against each other, with the acceleration timescale being some characteristic time for the particle to accelerated, and the escape timescale being a similar characteristic time for the particle to be ejected from the system. As long as the acceleration timescale is lower than the escape timescale, the particle will continue to be accelerated, but as soon as the escape timescale overtakes the acceleration timescale, acceleration ceases and the particle is lost. The characteristic timescale of the acceleration process depend on scattering centers N per unit volume with collision cross section σ and velocity of moving plasma boundary V_P.

Conclusion

Helium ion beam was detected using fast response charge collector system (Faraday cup) and time-integrated solid state nuclear track detector LR-115A. Faraday cup measurements showed that the ion energy spectrum a mixture of faster group of ions that has higher kientic energy ranging from 15 to 540 keV and slower group that has lower kientic energy value ranging from 0.3 to 1.0 keV. It is found that the ion flux depend on the filling gas pressure and the maximum ion flux was registered at P = 0.8 Torr of helium gas. The ion flux density has been determined using track etching techinque LR-115A. The flux desity of ion beam was estimated to be 4.4×10^{11} ion/steradian using CCZ model.

References

[1] Bernstein MJ (1970) Acceleration mechanism for neutron production in plasma focus and Z-pinch discharges. Phys Fluids 13:2858–2866
[2] Jager U, Herold H (1987) Fast ion kinetics and fusion reaction mechanism in the plasma focus. Nucl Fusion 27:407–423
[3] P asternak A, Sadowski M (1998) Analysis of ion trajectories within a pinch column of a PF-type discharge. In: Proc ICPP&25th EPS Conf CFPP. Praha, Czech Republic. ECA 22C:2161–2164
[4] M. Zakaullah *et al.*, Phys. Plasma **6**, 3188 (1999).
[5] Gerdin G, Stygar W and Venneri F 1981 J. Appl. Phys.52 3269-75
[6] J.W. Mather, Methods of Experiments Physics, ed H. Griem and R. Loverberg, **9B**, 187 (1971).
[7] R. Deutsch and W. Kies, Plasma Phys. Control. Fusion **30**, 263 (1988).
[8] G. Gerdin, W. Stygar and F.J. Venneri, J. Appl. Phys. **52**, 3269 (1981).
[9] H. Kelly and A. Marquez, Plasma Phys. Control. Fusion **38**, 1931 (1996).
[10] G. Gerdin, W. Stygar and F. J. Venneri: J. Appl. Phys. 52 (1981) 3269.

[11] C. S. Wong, P. Choi, W. S. Leong and J. Singh: Jpn. J. Appl. Phys. 41 (2002) 3943.
[12] H.R. YOUSEFI, Y. NAKATA, H. ITO and K. MASUGATA Characteristic Observation of the Ion Beams in the Plasma Focus Device, Plasma and Fusion Research, Volume 2, S1084 (2007)
[13] G M EL-Aragi, U Seddik and A Abd EL-Haliem, Detection of accelerated particles from pulsed plasma discharge using solid state nuclear track detector, Pramana Journal of Physics Vol. 68, No. 4, pp. 603-609; (2007).